Universidad Carlos III de Madrid
e-Archivo

Institutional Repository

This document is published in:

New Alloying Systems for Sintered Steels: Critical Aspects of Sintering Behavior

RAQUEL ORO, MÓNICA CAMPOS, CHRISTIAN GIERL-MAYER,
HERBERT DANNINGER, and JOSÉ MANUEL TORRALBA[*]

Oxygen-sensitive alloying elements such as Mn, Si, and Cr have a high potential for improving the properties of low alloyed sintered steels while reducing the alloying cost. However, it is necessary to find a way for avoiding, or at least minimizing, the oxidation of these elements especially during the early stages of the sintering cycle. In this study Mn, Si, and Cr were introduced in the form of a master alloy powder designed to be mixed with the iron base powder and provide the final composition of the steel during the sintering process. The reduction/oxidation phenomena taking place during the heating stage were studied by thermogravimetry, dilatometry, and mass spectroscopy, using either reducing (H_2) or inert (Ar) atmospheres. The results show how the difference in chemical activity between base iron powder and master alloy causes the so called "internal-getter" effect, by which the reduction of less stable iron oxides leads to oxidation of the elements with higher affinity for oxygen. This effect can be somehow minimized when sintering in H_2, since the iron oxides are reduced at lower temperatures at which the reactivity of the elements in the master alloy is lower. However, H_2 concentration in the processing atmosphere needs to be carefully adapted to the specific composition of the materials being processed in order to minimize decarburization by methane formation during sintering.

I. INTRODUCTION

POWDER metallurgy (PM) is a cost-effective process used, *e.g.*, for manufacturing near net-shape metallic products by die pressing metal powder into the desired shape and then consolidating the material by sintering at elevated temperatures. However, in the last years, the increasing cost and volatility in prices of the most common alloying elements in low alloy sintered steels (Cu, Ni, Mo), have been the motives for research into new alloying alternatives. Cheaper and more efficient alloying elements are Cr, Mn, and Si, widely used in the production of wrought steel parts. However, these elements present much higher affinity for oxygen than the traditional alloying elements. This is a very important limitation for the PM technology since the high

specific surface area available in the powder particles makes them more reactive in contact with the surrounding atmosphere and complicates the elimination of the natural oxides covering the powder particles. A possible way for avoiding oxidation is to introduce these elements combined (*i.e.*, alloyed) with other elements with a lower affinity for oxygen (for instance Fe).[1,2] In such way, the chemical activity of the oxidation-sensitive elements can be significantly reduced. This is the case with fully prealloyed iron powders. Cr and Mn have been so far introduced in sintered steels by the preal-loying route, and the characteristic oxidation/reduction stages taking place during the sintering process have been defined by the proper combinations of thermal analyses and degassing experiments.[3–6] In case of Cr-Mo prealloyed iron powders, this type of studies have been the key point for adapting the sintering procedures to the specific behavior of these materials which nowadays are being sintered successfully in the industry. Besides the prealloying route, another interesting approach is the master alloy concept. A master alloy can be defined as a powder with a high concentration of alloying elements designed to be mixed with an iron base powder and provide the desired final composition during the sintering cycle. This concept was first introduced in the 70s with the development of master alloys based on complex carbides.[2,7,8] Since then, several approaches have been made following this route, with some very promising results especially with Mn-containing master alloys.[9–14] Combination of Mn and Si in an Fe-Mn-Si master alloy was addressed for the first time in the 80s by Klein *et al.*[15–19] who obtained

*RAQUEL ORO, formerly with the Universidad Carlos III de Madrid, Av. Universidad 30, 28911 Leganés, Madrid, Spain, is now Post-doctoral Researcher, with the Chalmers University of Technology, Rännvägen 2A, 41296 Gothenburg, Sweden. Contact e-mail: raqueld@chalmers.se MÓNICA CAMPOS, Docent, is with the Universidad Carlos III de Madrid. CHRISTIAN GIERL-MAYER, Senior Researcher, and HERBERT DANNINGER, Full Professor, are with the Institute of Chemical Technologies and Analytics, Vienna University of Technology, Getreidemarkt 9/164-CT, 1060 Vienna, Austria. JOSÉ MANUEL TORRALBA, Full Professor, is with the Universidad Carlos III de Madrid, also with the IMDEA Materials Institute, c/Eric Kandel, 2, 28906 Getafe, Madrid, Spain.
From 12th January 2015, Raquel de Oro Calderon will be at Vienna University of Technology.

mechanical properties that still today belong to the best data available for as-sintered materials, with the added value of showing extremely low dimensional changes. However, in spite of their high level of properties, Mn-Si master alloys not only did not reach the market but have also disappeared for some years from the research areas mostly as a consequence of inadequate furnace technology and insufficient atmosphere quality.

The aim of the work presented here is to understand the peculiarities introduced in the sintering processes by the simultaneous presence of Mn and Si (and in some case Cr) in the form of a master alloy. The master alloy powders used were specifically designed to enhance sintering by the formation of a liquid phase, and therefore their compositions are adjusted towards low liquidus temperatures.[20] Three master alloy powders with slightly different compositions (Fe-Mn-Si, Fe-Mn-Si-C, and Fe-Mn-Si-C-Cr-Ni) were studied with the aim of understanding the influence of different alloying elements in the reduction–oxidation reactions: First the reduction stages typical of the gas atomized master alloy powders were studied, and then, thermal analyses were performed on different steel green compacts containing master alloy additions. The study is mainly focused on understanding the deviations from the natural degassing-reduction behavior of the base iron powder as a consequence of the presence of alloying elements with high oxygen affinity locally concentrated in the master alloy particles.

II. MATERIALS AND EXPERIMENTAL PROCEDURE

The characteristics of the materials used in the different experiments are summarized in Table I. Master alloy powders with the composition given in Table I were obtained by gas atomizing in N_2 (purity 99.9 pct) using a lab scale atomizer (Atomizing System LTD). The oxygen content of the master alloy powder after atomizing is below 0.04 wt pct.

Thermoanalytical studies were carried out by thermogravimetry and dilatometry analyses coupled, in certain experiments, with mass spectrometry. The equipments used for the different thermoanalytical studies are gathered in Table II together with the characteristics of the different experiments. In those experiments where the mass spectrometer was coupled the masses detected were: 12(C), 14(N), 15(CH_3), 16(CH_4, O), 17(OH), 18(H_2O), 28(CO, N_2), 32(O_2), and 44(CO_2).

The thermal behavior of the three different master alloy powders was studied by thermogravimetric analyses (TGA) carried out in a Setsys Evolution TGA–DTA thermal analyzer. Loose master alloy powders were used in these experiments, with or without additions of admixed graphite (0.6 wt pct). Admixed graphite has been added in these experiments in order to study its effect as reducing agent and to identify the temperatures "windows" for reduction. Shifting in the melting temperature of the master alloys as a consequence of the addition of graphite has been previously studied and the results showed that this shifting is only relevant for master alloy powders which do not contain carbon in their initial composition.[20] The same amount of graphite was added to all master alloy powders, meaning that, for those master alloys which contain carbon in their initial composition, the total final carbon content in the mix is higher.

With the aim of analyzing the effect of the interaction between the iron base powder and the master alloy, thermogravimetric experiments were carried out on green compacts pressed at 600 MPa containing water atomized iron powder ASC 100.29 admixed with 0.6 wt pct graphite and with increasing amounts (0, 4, 20 wt pct) of master alloy MA2.

The effect of the chemical composition of the base iron powder was studied by TGA carried out on green compacts pressed at 600 MPa containing three different iron base powders (Water atomized, carbonyl or prealloyed, see Table I) admixed with 0.6 wt pct graphite and with increasing amounts of master alloy MA2 (0, 4,

Table I. Summary of the Materials Used in the Different Studies

Master alloys	MA1: Fe-40Mn-17Si (wt pct), sieved < 45 μm, d_{50} ~ 20 μm
	MA2: Fe-40Mn-15Si-1C (wt pct), sieved < 45 μm, d_{50} ~ 20 μm
	MA3: Fe-40Mn-15Si-1C-5Cr-10Ni (wt pct), sieved < 45 μm, d_{50} ~ 20 μm
Graphite	natural graphite (grade UF4, Kropfmühl)
Iron base powder	water atomized iron powder (grade ASC 100.29, Höganäs AB Sweden)
	O < 0.08 wt pct, C < 0.01 wt pct
	carbonyl iron powder (grade OM, BASF SE)
	O: 0.15-0.40 wt pct, C: 0.75-0.90 wt pct, N: 0.65-0.90 wt pct
	prealloyed iron powder (grade Astaloy CrM Höganäs AB Sweden)
	Cr: 3 wt pct, Mo: 0.5 wt pct, O < 0.25 wt pct, C < 0.3 wt pct

Table II. Equipments Used for Thermal Analyses

Equipment	Mass Spectrometer Coupled	Experiment Characteristics
Thermal Analyzer TGA-DTA Setsys Evolution (Setaram)	Pfeiffer Omnistar 1-300 UMA	Ar, 1573 K (1300 °C) 1 h, heating and cooling rate 10°/min
Dilatometer Netzsch 402 C	QMS 403 Aeölos	Ar or H_2, 1573 K (1300 °C) 1 h, heating and cooling rate 10°/min

20 wt pct). In these experiments, a mass spectrometer Pfeiffer Omnistar1-300 UMA was coupled to the thermal analyzer.

The effect of the atmosphere in the reduction/oxidation reactions was studied by dilatometry analyses in a Netzsch 402 C dilatometer coupled with a QMS 403 Aeölos mass spectrometer using either an inert (Ar) or reducing (H_2) atmosphere. For these experiments green compacts pressed at 600 MPa containing water atomized iron powder mixed with 0.6 wt pct graphite and 4 wt pct master alloy powder were used. Purity of the gases used in all studies was 99.999 pct, and the oxygen content was below 2 ppm.

As a rule, in a conventional processing route of PM components, solid lubricants (such as microwax or stearates) are added to facilitate the pressing step. To avoid the effect of the delubrication stages, no lubricant was added in the initial mixes. Mass losses (pct) are therefore calculated directly from the difference between the mass of the green compact and the mass of the sample sintered in the dilatometer.

In order to obtain information about the effect of the atmosphere on the final interstitial content (carbon and oxygen), the samples obtained from dilatometry experiments were dry-cut manually in pieces of approximately 600 mg. Oxygen content was measured with a LECO-TC500 equipment, and carbon was analyzed using a LECO-CS200.

Sections of the samples sintered in the dilatometer were prepared following the conventional metallographic process using a mix (1:1) Nital 2 pct-Picral 4 pct as etching agent for optical microscopy examination.

III. RESULTS

A. *Thermal Analyses on Master Alloy Powders*

Thermogravimetry analyses carried out on loose master alloy powders with or without graphite additions allow identifying different mass losses during the thermal cycle. Figure 1 shows both the thermogravimetry curve and its derivative, which provides precise information about the temperature range within which the mass loss is taking place.

The experiments were carried out under inert (Ar) atmosphere. Therefore, in absence of carbon, there are no reducing agents available in the system. This is clearly seen in the curves corresponding to the master alloy without graphite additions, where no significant mass losses are registered. Not even master alloys MA2 and MA3, which contain 1 wt pct C on its initial composition, show any important mass losses in the temperature range studied. This suggests that carbon introduced in the initial composition of the master alloy is not efficiently acting as a reducing agent, and admixed graphite seems to be needed for achieving significant reduction of the oxides. This is most likely a consequence of the lower chemical activity of prealloyed carbon at the range of temperatures considered in this study.[21,22]

The approximate temperatures where the reductions are taking place, together with the mass losses detected on each stage, are presented in Table III. Three reduction stages can be defined for MA1 and MA2 admixed with 0.6 wt pct graphite, and the temperature ranges are very similar for both master alloys. The first reduction
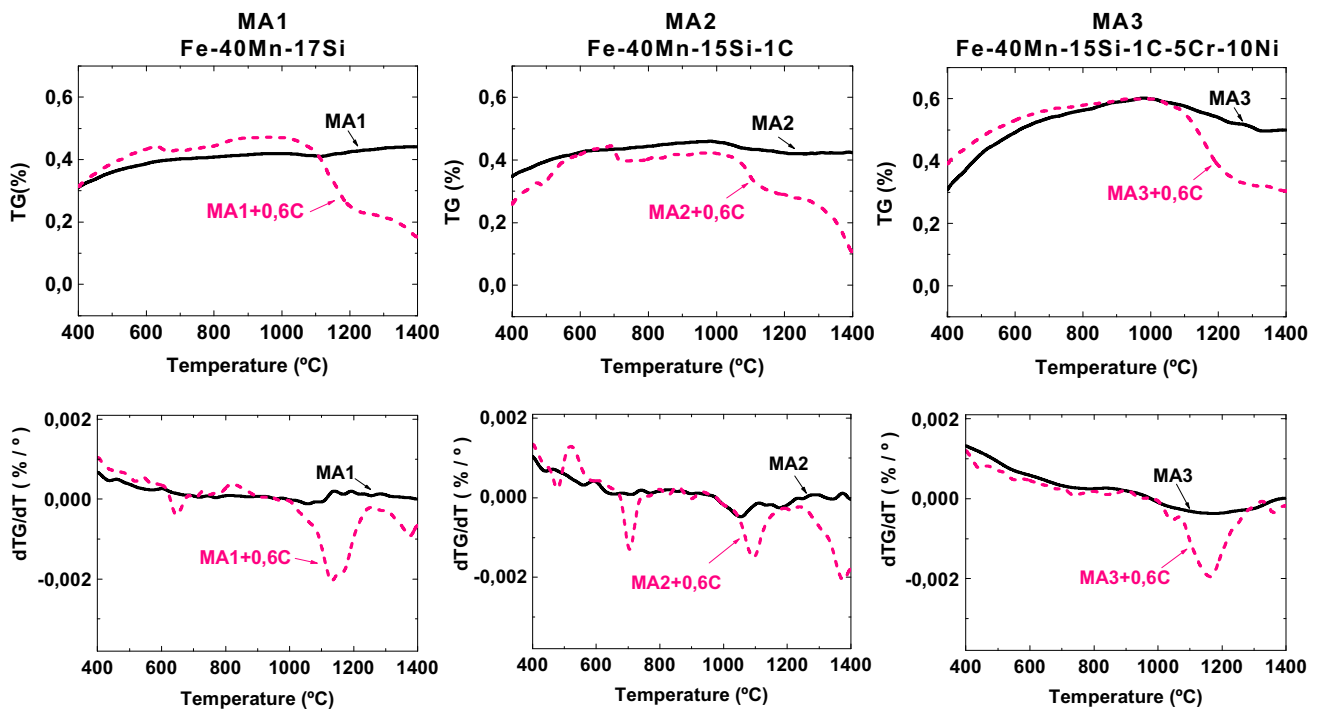

Fig. 1—Thermogravimetry curves and their derivatives for master alloy powders with and without graphite additions. Analyses carried out under Ar atmosphere.

stage takes place at temperatures around 973 K (700 °C) and is characteristic of the carbothermal reduction of less stable surface iron oxides.[6,23–29] The second and third reduction stages represent the most important mass losses and are most likely linked to the reduction of highly stable Mn-Si containing oxides.

The reduction stages found are in agreement with the studies describing the chemical composition and morphology of the master alloy particles surface. As has been previously reported, the surface of these master alloy particles is heterogeneous and consists of a thin iron oxide layer, covering most of the surface, in which some clusters containing a fine dispersion of Mn-Si particulate oxides are found.[30] The first reduction stage should therefore correspond with the reduction of the thin iron oxide layer, and the second and third stage suggests the presence of at least two types of Mn-Si oxides with different thermal stability.

As the amount of alloying elements with high oxygen affinity (Si, Mn, Cr) increases (MA2 < MA1 < MA3), the intensity of the low temperature reduction peak decreases (see Figure 1), and disappears completely for master alloy MA3 (the only Cr-containing master alloy). A similar effect was previously reported for prealloyed iron powders containing Cr, for which the reduction stages typical of plain iron powders disappeared, and the reduction processes were shifted to higher temperatures. In Cr-prealloyed powders this phenomenon has been associated with a transformation of less stable iron oxides into more stable (Cr-containing) oxides.[5,24] Recent studies have proved that such transformation occurs through the formation of Fe-based spinels (Fe_2MnO_4 and $FeCr_2O_4$). When Cr and Mn are simultaneously present, reduction of the iron part of Fe-based spinels leads to formation of Cr-Mn spinels (most likely the type $MnCr_2O_4$) that can only be reduced at temperatures above 1373 K (1100 °C).[31,32] Such evolution is in perfect agreement with the results obtained for master alloy MA3, for which reduction reactions are only detected at temperatures above 1373 K (1100 °C).

Table III. Mass Loss (in Percent) Detected at Different Temperatures in Thermogravimetric Analyses Performed on Mixes Containing Master Alloy and 0.6 wt pct Graphite

	Mass Loss		
Stage	T (K)	T (°C)	Δm (pct)
MA1 + 0.6C			
I	~923	~650	−0.02
II	1373 to 1473	1100 to 1200	−0.2
III	~1643	~1370	−0.1
MA2 + 0.6C			
I	~973	~700	−0.05
II	~1373	~1100	−0.1
III	~1643	~1370	−0.2
MA3 + 0.6C			
I	—	—	—
II	~1433	~1160	−0.3
III	—	—	—

B. Thermal Analyses on Steel Compacts Modified with Master Alloy Additions

Figure 2 shows the thermogravimetric curves of green compacts containing water atomized iron powder admixed with increasing amounts of master alloy MA2. The reduction stages typical of the iron base powder are clearly seen in the thermogravimetry curve—Fe + 0.6C—and have been previously described by other authors to evolve as follows: The first reduction stage at approximately 973 K (700 °C) corresponds with the carbothermal reduction of iron surface oxides. Afterwards, a second mass loss starting at approximately 1273 K (1000 °C) is associated with the reduction of more stable oxides, or internal oxides (including those trapped in the sintering contacts) that require higher temperatures to diffuse to the surface.[3,23–28]

As shown in Figure 2, when increasing amounts of master alloy are added to the base powder (4 or 20 wt pct), the mass loss registered in the first reduction stage—at 973 K (700 °C)—progressively decreases, and the high temperature mass losses are shifted to higher temperatures—the signal becomes more similar to the one registered in the master alloy powder (MA2 in Figure 1).

A similar effect is observed for the two iron base powders studied—water atomized iron and carbonyl iron powder (Figure 3). Figure 3 shows the influence of the base powder composition on the reduction/oxida-tion reactions. Both the derivative of the thermogravi-metry curve and the signals of mass m28 (CO) are represented, and the fact that these two signals are symmetrical confirms that the mass losses registered are related with the carbothermal reduction of oxides.

Considering the curves for water atomized iron, the more master alloy is added to the mix, the more similar the reduction stages are to those characteristic from the master alloy powder. With high master alloy contents (20 wt pct), the CO peak at 973 K (700 °C) is almost completely absent, which suggest that the CO generated from the carbothermal reduction of the oxides might be immediately reacting with the master alloy particles.[33]

A similar trend is observed in the temperature range between 873 K and 1673 K (600 °C and 1400 °C) for steels containing carbonyl iron base powder (see detail in Figure 4), when increasing the amount of master alloy, the first reduction stage at 873 K and 973 K
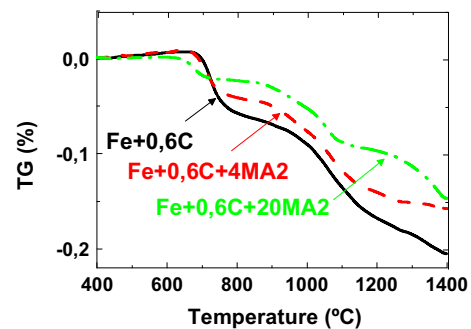

Fig. 2—Thermogravimetry curve for steels containing increasing amounts of master alloy MA2 analyzed under Ar atmosphere.
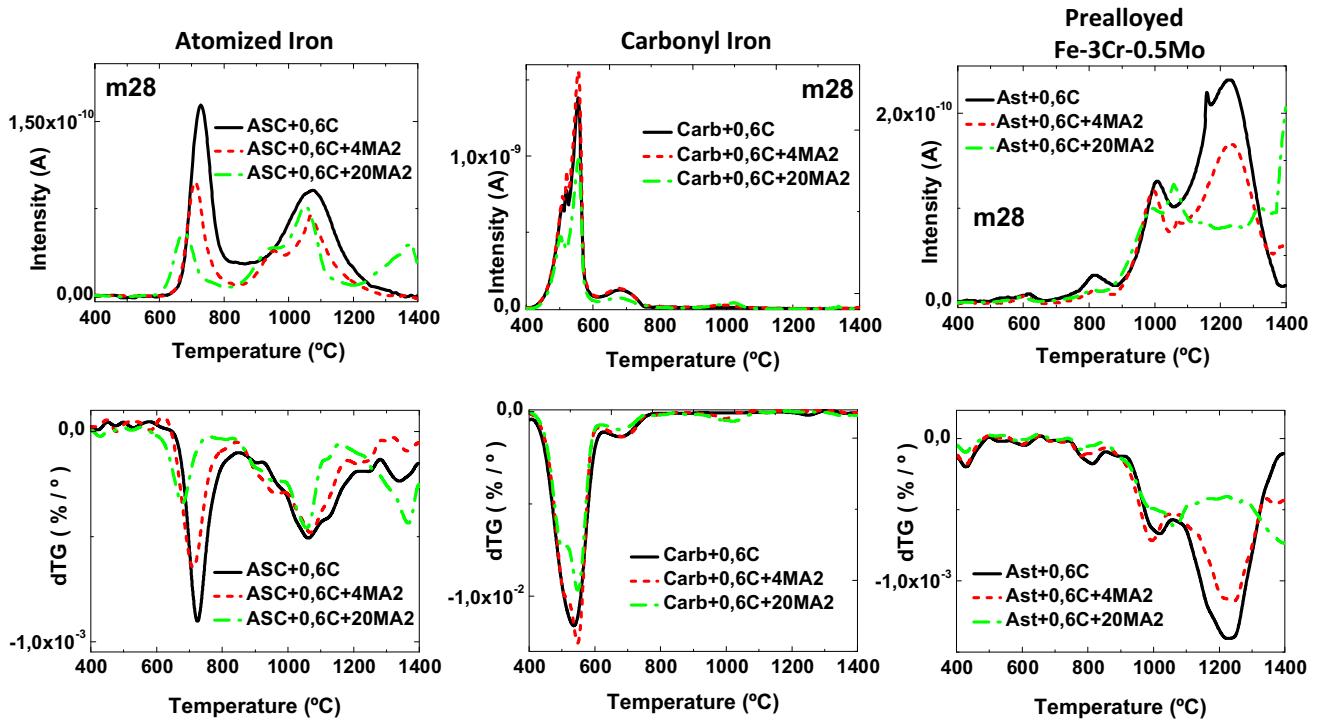
Fig. 3—Thermal analyses under Ar atmosphere of steels containing master alloy MA2. Up: degassing curve for mass 28 (CO). Down: derivative of the thermogravimetry curve.
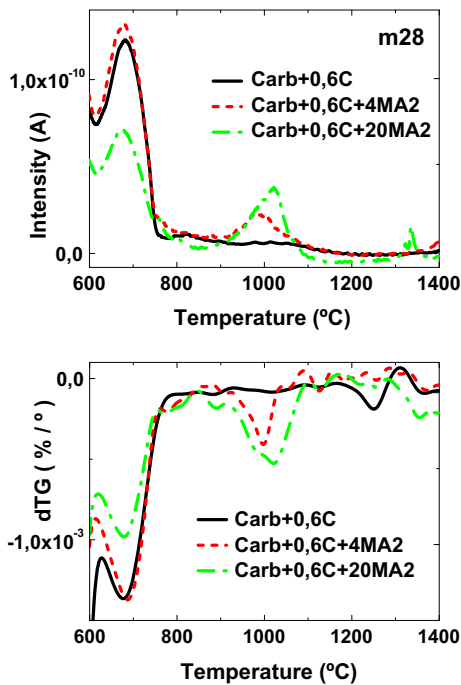

Fig. 4—Detail of the thermal analyses for steels containing carbonyl iron base powder admixed with master alloy MA2, in the temperature range 873 K to 1673 K (600 °C to 1400 °C). Up: degassing curve for mass 28 (CO). Down: derivative of the thermogravimetry curve.

(600 °C and 700 °C) decreases in intensity, and the reduction peaks become more similar to those typical of the master alloy powder. A very intense peak of mass 28 is registered in steels containing carbonyl iron powder in the range of temperatures between 673 K and 873 K (400 °C and 600 °C). Carbonyl iron powders are produced by decomposition of iron pentacarbonyl at approximately 523 K and 573 K (250 °C and 300 °C), using small amounts of ammonia as catalyst. As the iron grows it can trap or absorb CO and N_2 and, due to the low processing temperatures, these elements have little energy available to cause the formation of compounds and therefore remain loosely bonded or trapped in the lattice.[34] Therefore, the peak observed in mass 28 (CO or N_2) in the low temperature range—673 K and 873 K (400 °C and 600 °C)—is more likely related with desorption of such species than with an oxide reduction process, since the temperature is too low for the reduction of iron oxides.

When using Cr-prealloyed base powder (Figure 3), the reduction peaks typical of the base powder are modified as well. However, in this case, when high amounts of master alloys are added to the base powder the third reduction stage is shifted to even higher temperatures than in the other two cases, which suggests an increase in the amount of highly stable oxides.

C. Thermal Studies in Different Atmospheres

Better understanding of the different oxidation/reduction reactions can be gained from studying the degassing processes under different atmospheres. With that aim, dilatometry analyses coupled with mass spectrometry were performed under inert (Ar) or reducing (H_2) atmospheres on steel compacts containing small additions (4 wt pct) of master alloys MA1, MA2, and MA3.

Figure 5 shows the different dilatometry curves together with the most relevant gaseous species detected on each atmosphere.

In Ar atmosphere (left column in Figure 5) two clear stages can be defined. First, the CO peak at temperatures around 873 K to 973 K (600 °C to 700 °C) indicates the reduction of the less stable iron oxides. Next, starting at approximately 1273 K (1000 °C), there is a second reduction stage indicated by a broad CO signal with peaks around 1373 K and 1473 K (1100 °C and 1200 °C). This latter peak is not completely registered even after sintering at 1573 K (1300 °C), and is probably related to the reduction of very stable Mn-Si oxides.

Compared with previous studies on the typical reduction peaks of water atomized iron base pow-der,[3,23–28] the addition of small amounts of master alloy (only 4 wt pct) lowers considerably the intensity of the first reduction peak.

When sintering in reducing atmosphere, H_2 (right column in Figure 5), reduction of iron oxides at temperatures around 673 K (400 °C) is evidenced by the m18 (H_2O) peak. However, the reduction of more stable oxides necessarily takes place through carbothermal reaction, since carbon is the most effective reducing agent at the higher temperatures needed for their reduction.[3] This second reduction stage occurs at approximately the same temperatures as those observed in Ar atmosphere—peaks at 1373 K and 1473 K (1100 °C and 1200 °C)—and again, the signal is not completely registered at 1573 K (1300 °C), which indicates that the reduction should continue at even higher temperatures.

A peculiar event occurring when sintering in H_2 is the generation of methane (CH_4) at temperatures around 1023 K (750 °C) which is evidenced by a peak with mass 16, and is confirmed by the presence of a mass 15 curve parallel to that of mass 16.
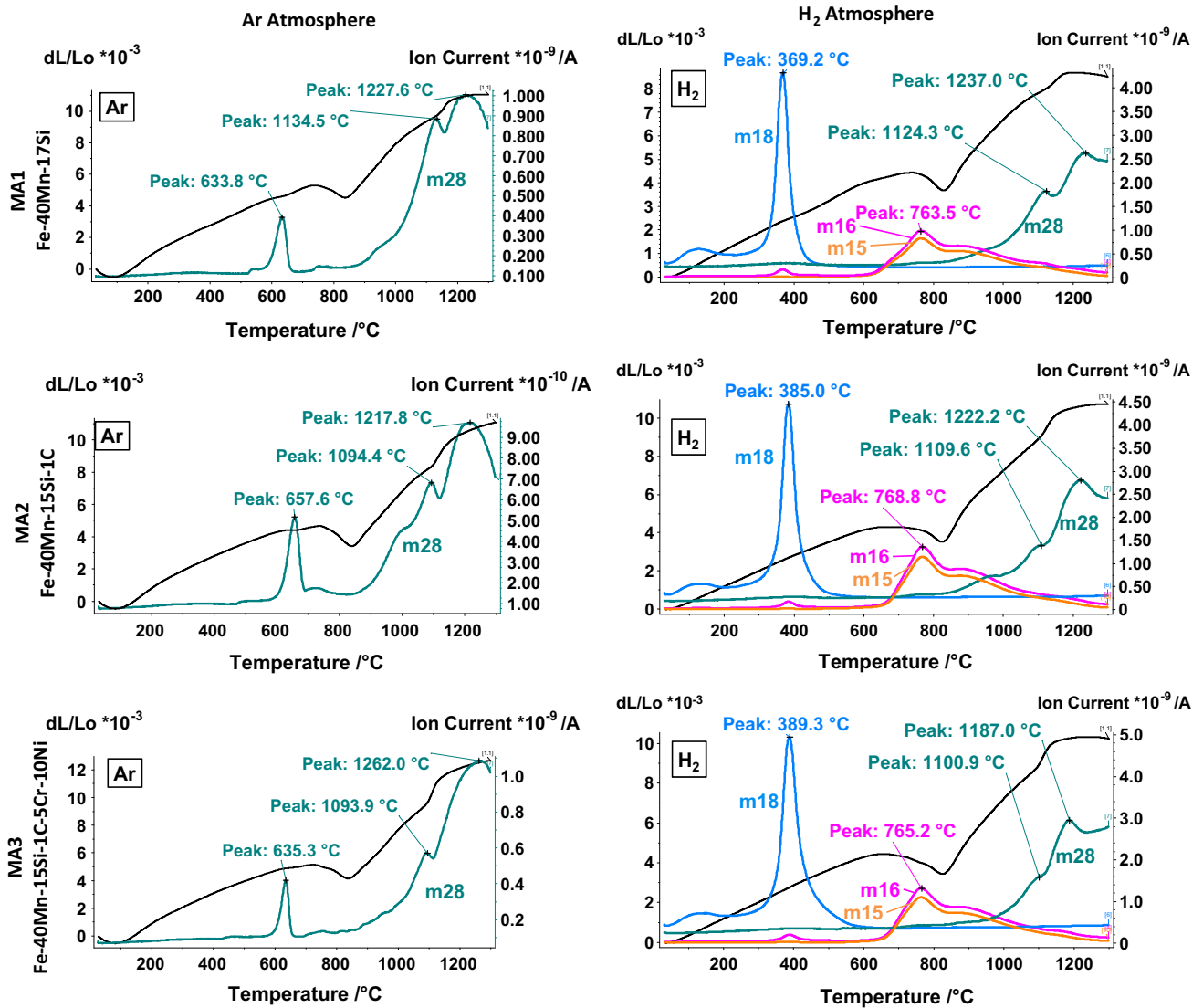

Fig. 5—Dilatometry and gas formation curves during sintering of steel compacts with a composition Fe-0.6C-4MA (wt pct) for master alloys MA1, MA2, and MA3. The experiments were performed either in inert (Ar) or reducing (H_2) atmosphere.

Chemical analyses carried out after dilatometry experiments (Table IV) show lower oxygen contents in the samples sintered in H_2, which is a consequence of the efficient reduction of iron oxides at lower temperatures, complemented by the carbothermal reduction at higher temperatures. When sintering in H_2, the most efficient reduction of oxides by H_2 at lower temperatures generally leads to less carbon consumption by carbothermal reactions.[3] However, for the three master alloys studied, carbon losses are considerably higher in samples sintered under H_2 atmospheres (Table IV), most likely due to the consumption of carbon by the CH_4 formation detected in these experiments. Enhanced decarburization in H_2 atmosphere is evident in the microstructure of steels containing MA1, which presents the highest Si content (Figure 6).

IV. DISCUSSION

There are basically two effective ways of introducing elements with a high oxygen affinity in sintered steels (Figure 7): by the use of completely prealloyed iron powders or by mixing a plain iron base powder with a "master alloy powder" (a powder which contains all of the alloying elements in a combined form). The master alloy route presents interesting advantages compared to prealloyed such as the possibility to maintain the compressibility of the base powder, and the higher flexibility in the selection of the final composition.[6,33,35–37] Besides, it is possible to specifically tailor the composition of the master alloy to promote the formation of a liquid phase that enhances the sintering process.

Both prealloying and master alloy routes allow reducing the chemical activity of the oxygen-sensitive elements. However, when using master alloys, the chemical activity of the base iron powder and master alloy powder is different—heterogeneous chemical activity in the powder mix. Thus, each component will undergo its own reduction process that will depend on its chemical and morphological characteristics. Such heterogeneity in chemical affinity can promote an oxygen transfer between the different powder particles which, as has been shown in Figures 3 and 5, is taking place through the sintering atmosphere—"internal gettering effect".[33] In the context of this study, "Internal gettering" means oxygen transfer from the oxide of a metal with low oxygen affinity (*e.g.*, Fe) to a metal with higher oxygen affinity (*e.g.*, Mn) through the gas phase, in the present case through the pores of a powder compact.[38] This is in contrast to "scavenging", which means oxygen transfer within a solid or liquid metal through diffusion processes in the metallic phase.[39]

The internal-getter effect is depicted in Figure 8 for the case of the direct carbothermal reduction reaction (Eq. [1]). At those temperatures at which the carbothermal reduction of iron oxides is likely to occur—873 K to 973 K (600 °C to 700 °C), the conditions might be reducing for Fe but strongly oxidizing for elements such as Mn and Si.[33] Thus, the direct carbothermal reduction—Eq. [1]—takes place to the right side (reduction) for the iron oxides and to the left side (oxidation) for Mn and Si metallic species present in the master alloy. The overall effect is that reduction of iron oxides leads to the oxidation of Mn and Si and therefore there is no
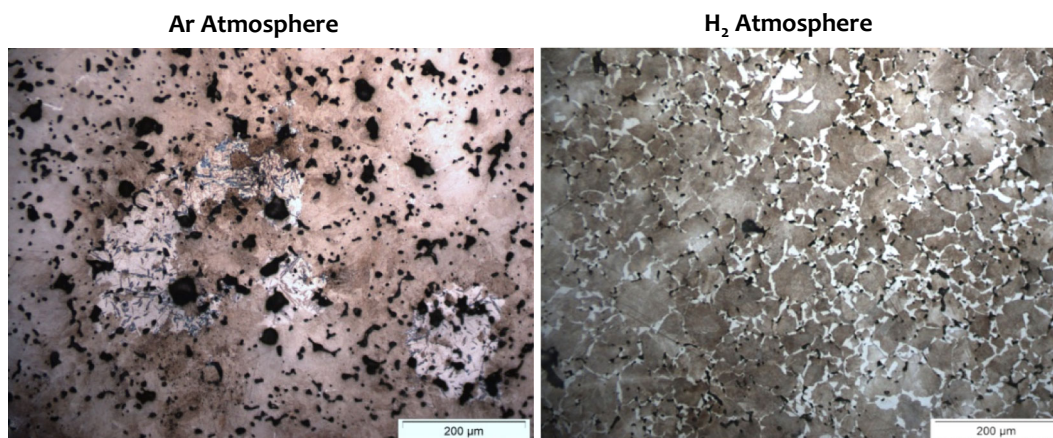
Table IV. Mass Losses and Carbon and Oxygen Contents Measured After Dilatometry Experiments

	O (wt pct)	C (wt pct)	Carbon Loss (pct)	Mass Loss (pct)
MA1				
Ar	0.025	0.43	0.17	0.27
H_2	0.013	0.31	0.29	0.35
MA2				
Ar	0.031	0.44	0.20	0.24
H_2	0.026	0.39	0.25	0.34
MA3				
Ar	0.031	0.49	0.15	0.28
H_2	0.023	0.42	0.22	0.32

Carbon losses have been calculated as the difference between the total combined carbon added to the initial mix (considering both the admixed graphite and the carbon content in the master alloy) and the combined carbon measured after the experiments.

Ar Atmosphere **H₂ Atmosphere**

Fig. 6—Metallography of dilatometry samples containing MA1 sintered under Ar (left) and H_2 (right) atmospheres. Etching agent Nital 2 pct-Picral 4 pct.
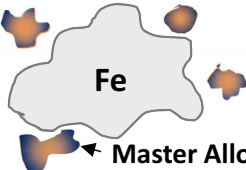
	PREALLOYING ROUTE	**MASTER ALLOY ROUTE**
Chemical Activity	Low and constant (homogeneous) chemical activity of oxidation sensitive elements	Chemical activity depends on the master alloy composition. Differences in chemical activity between base powder and master aloy (heterogeneous)
Compressibility	Lower than in mixes, but in part compensated by shrinkage in sintering	Small master alloy additions allow preserving the compresibility of the base powder.
Flexibility	Fixed compositions	Composition can be tailored by modifying the amount of master alloy added, or by using different base powders.
Homogeneity of alloying elements	Fully homogeneous microstructures	Homogenization depends on diffusion rate of alloying elements in the base powder. It can be improved by designing master alloys that form a liquid phase.
Cost	High price in comparison with the common iron grades	Expensive if fine powder fractions are to be used. Added in small amounts the overall effect in price can be limited.

Fig. 7—Characteristics of the two most relevant alternatives to introduce elements with high oxygen affinity: prealloyed or master alloy route[6,33,35–37].

net mass loss, since oxygen is at least partly transferred from the surface of the base powder to the surface of the master alloy particles. This, in turn, means that even at high temperatures, high concentration of CO imply an important risk of oxidation for the oxygen-sensitive elements if the temperature is still not high enough to enable reduction by the direct carbothermal reaction, *i.e.*, if the equilibrium of (Eq. [1]) is still on the side of the metal oxide. Of course the same holds for the indirect reduction (Eq. [2]), in this case CO_2 being the oxidizing agent

$$yC + Me_xO_y \leftrightarrow xMe + yCO(g), \qquad [1]$$

$$yCO(g) + Me_xO_y \leftrightarrow xMe + yCO_2(g). \qquad [2]$$
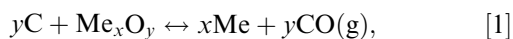
Interaction between master alloy particles and base powder has been studied considering different types of base powders: plain iron (water atomized or carbonyl iron powder) and prealloyed iron (Fe-3Cr-0.5Mo). When Cr-prealloyed powder is used (right column in Figure 3), as the amount of master alloy added increases, the reduction peaks at temperatures around 1473 K (1200 °C) progressively disappear, and the reduction is shifted to higher temperatures. The inter-esting fact is that these temperatures are even higher than those found in mixes containing plain iron base powder, even though Cr-containing oxides should not have higher stability than the Mn-Si oxides that can be formed as well with a plain iron base powder. The fact

that the peaks are shifted to higher temperatures reveals a higher contribution of oxides with the highest stability, which in the systems considered in this work should be Mn-Si or Si oxides (according to the Ellingham diagram presented in Figure 9). But, why should the contribution of highly stable Mn-Si or Si oxides be higher when the Fe-Mn-Si master alloys are mixed with Cr-prealloyed powders instead of plain iron powders? A possible explanation to this effect is the shift in the temperature range at which the internal-getter effect takes place. When using plain iron base powders, the internal-getter effect occurs in the range of temperatures where its surface oxides (mainly iron oxides) are reduced, leading to the formation of any of the oxides with a higher stability (any of the lines that are below the Fe-oxides in the Ellingham diagram in Figure 9). However, as previously reported by other authors, in Cr-prealloyed powders at least part of the oxygen is trapped due to the transformation of oxides ($Fe_2O_3 \rightarrow FeO \rightarrow Fe\text{-}Cr_2O_4 \rightarrow MnCr_2O_4$).[31,32] The internal-getter effect de-scribed for plain iron powders can take place as well when using Cr-prealloyed base powders, but only at the higher temperatures needed for reducing the highly stable Cr-Mn spinel oxides—above 1373 K (1100 °C). At such higher temperatures the kinetic of the internal-getter effect is faster, and the only oxides that can be formed are the most stable ones (Si containing oxides).Therefore, their contribution will be more important than when using plain iron base powders.

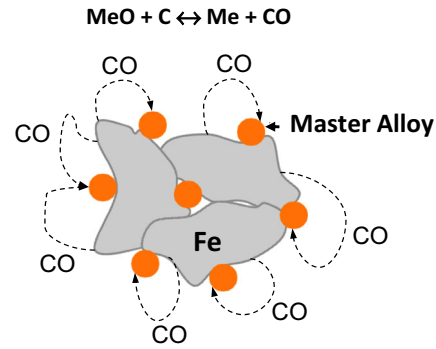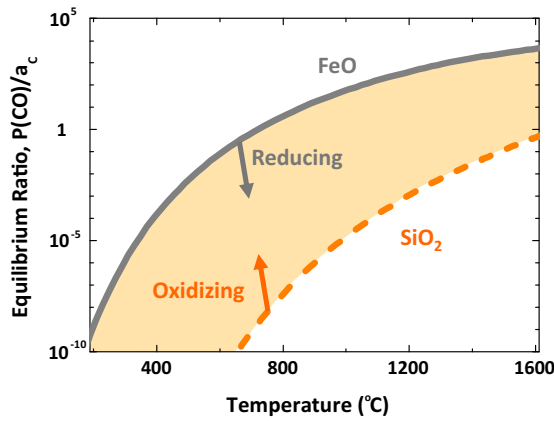The differences observed between mixes containing plain iron powder or Cr-prealloyed powder can then be

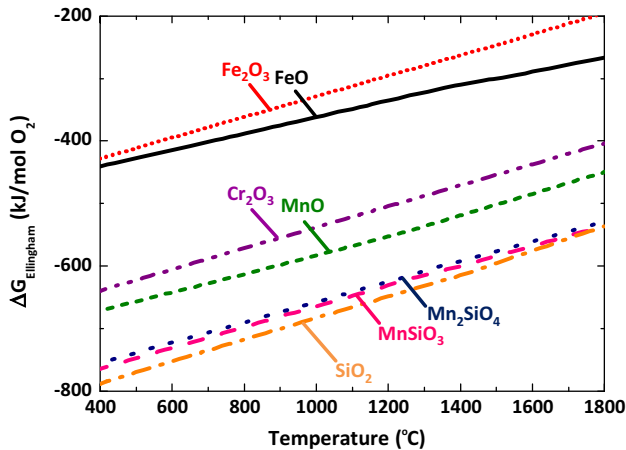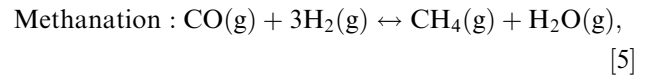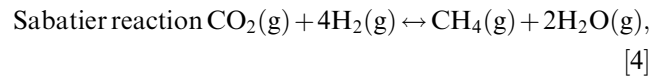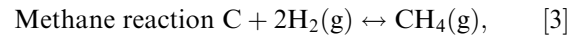Fig. 8—Schematic of the "internal getter" effect.

Fig. 9—Ellingham diagram for some of the possible oxides present in the systems studied. Thermodynamic data were calculated with the software HSC Chemistry 4.1.

related both with the kinetics of the internal-getter effect, and with the type of oxides that can be formed in the temperatures range in which the internal-getter effect takes place. As reported by other authors, Mn-Cr spinel oxides ($MnCr_2O_4$) should lie between the lines of Cr_2O_3 and MnO in the Ellingham diagram represented in Figure 9. As can be observed in Figure 9 there is a significant difference in stability of Mn-Cr oxides and Mn-Si or Si oxides which can cause the internal-getter effect. At those temperatures where Cr-Mn and Mn oxides are reduced, oxygen transfer occurs more readily since the master alloy particles can be expected to be more reactive, leading to the formation of Mn-Si or Si oxides.

The use of H_2 as reducing agent, very common when sintering steel components, allows an effectively reduction of iron oxides at temperatures around 673 K (400 °C). Thus, the "internal-getter" effect can be somehow avoided or at least alleviated since the reactivity of the master alloy at these lower temperatures is still rather low.

A very interesting and peculiar effect found when sintering in H_2 steels containing Fe-Mn-Si master alloys, is the formation of CH_4 in the intermediate temperature

range between 973 K and 1173 K (700 °C and 900 °C). Some possible reactions leading to methane generation through the interaction between the gasses present in the atmosphere are the following:

$$\text{Methane reaction } C + 2H_2(g) \leftrightarrow CH_4(g), \quad [3]$$

$$\text{Sabatier reaction } CO_2(g) + 4H_2(g) \leftrightarrow CH_4(g) + 2H_2O(g), \quad [4]$$

$$\text{Methanation}: CO(g) + 3H_2(g) \leftrightarrow CH_4(g) + H_2O(g), \quad [5]$$

$$2CO(g) + 2H_2(g) \leftrightarrow CH_4(g) + CO_2(g). \quad [6]$$

The Gibbs free energy of these reactions calculated at various temperatures using the software tool HSC Chemistry v4.0 is represented Figure 10. The fact that the Gibbs free energy for all these reactions is positive in the temperature range considered—973 K to 1173 K (700 °C to 900 °C)—makes them rather unlikely to occur.

Formation of CH_4 during steel sintering has never been reported before for Fe-C steels sintered in H_2,[3–6] which might indicate that the significant CH_4 formation found in these experiments is somehow linked with the presence of elements with a high affinity for oxygen. Thus, CH_4 formation could be related with the oxidation of strong oxide formers. The strongest oxide former in these systems is Si, which is also a rather unknown element in low alloy sintered steels. A possible reaction mechanism is that presented in Eq. [7] which implies the reaction of solid metallic species with H_2 and CO gaseous species from the atmosphere with the subsequent oxidation of metal and methane generation.

$$(x/y)Me + 2H_2(g) + CO(g) \leftrightarrow CH_4(g) + (1/y)Me_xO_y. \quad [7]$$
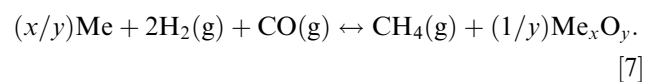
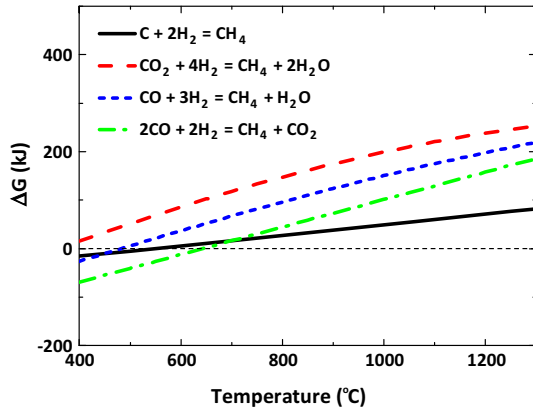Figure 11 represents the Gibbs free energy for the formation of different oxides through the reaction

Fig. 10—Gibbs free energy of possible reactions leading to methane formation through interactions between the gases present in the atmosphere. Thermodynamic data calculated with the software HSC Chemistry 4.1.
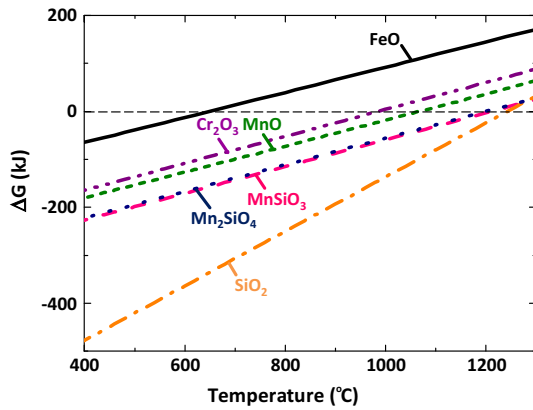

Fig. 11—Gibbs free energy of possible reactions leading to methane formation through reaction between solid and gaseous species: oxidation of strong oxide formers. Thermodynamic data calculated with the software HSC Chemistry 4.1.

proposed in Eq. [7] and reveals that most of them (except for the FeO formation) would occur spontaneously in the temperature range in which the methane peak was detected in this study—~1023 K (750 °C). Although the Gibbs free energy of these reactions is even more negative at lower temperatures, it is exactly in the temperature ranges where methane was detected in these studies that the Boudouard's equilib-rium—Eq. [8]—moves towards CO formation. Besides, it is approximately the same temperature where direct carbothermal reduction of iron oxides usually takes place. Formation of CO in this temperature range might then activate the formation of methane following Eq. [7].

$$C + CO_2(g) \leftrightarrow 2CO(g). \qquad [8]$$
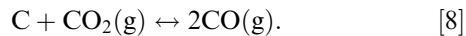
The reaction proposed in Eq. [7] involves the formation of methane by the oxidation of strong oxide former metals. According to Figure 11, in the temperature range where methane was detected, any of the oxides considered could be formed following this reaction
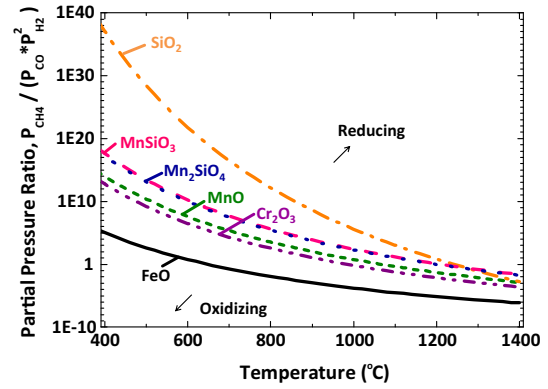

Fig. 12—Equilibrium conditions of temperature and partial pressure ratio P_{H_2}/P_{H_2O} between a metal and its oxide for different metallic systems. Below the curve the conditions favor the formation of the oxide and above the curve reduction is promoted. Thermodynamic data calculated with the software HSC Chemistry 4.1.

(except for FeO). SiO_2 formation is the most likely scenario, followed by the formation of mixed Mn-Si oxides and then MnO and Cr_2O_3. This might explain the fact that the formation of CH_4 has only been detected to an important extent when Si has been introduced in low alloy steels.

The conditions needed in the atmosphere for the reaction in Eq. [7] to evolve in one side or another are represented in Figure 12 as a function of temperature and $P_{CH_4}/\left(P_{CO} * P_{H_2}^2\right)$ ratio. Due to power of two of the P_{H_2} term, the use of diluted H_2—with the consequent reduction in P_{H_2}—should have the most significant effect in avoiding methane formation through Eq. [7]. Also small additions of CH_4 to the sintering atmosphere should help to reduce the $P_{CH_4}/\left(P_{CO} * P_{H_2}^2\right)$ ratio, avoiding the carbon losses apparently associated with the methane reaction in Eq. [7].

V. CONCLUSIONS

Oxidation-sensitive elements such as Mn, Si, and Cr have been introduced in low alloy sintered steels through the master alloy route, obtaining sintered materials with oxygen contents below 0.03 wt pct. Thermal analyses allowed identifying some of the peculiarities that need to be considered when sintering these materials:

1. Reduction of the oxides present in the master alloy powders takes place in three reduction stages. The first one—at approximately 873 K to 973 K (600 °C to 700 °C)—corresponds with the reduction of the thin iron oxide layer covering most of the surface of the master alloy particles. The second and third stages take place, respectively, between 1373 K and 1473 K (1100 °C and 1200 °C) and at temperatures above 1573 K (1300 °C), and provide the most important mass reduction, which suggests that most of the oxygen is combined forming stable oxides. Graphite admixed to the master alloy powder is needed to promote oxide reduction—even when car-

bon is present in the initial composition of the master alloy—which indicates that the activity of carbon prealloyed in the master alloy powder is too low for activating the reduction.

2. The heterogeneity in the oxygen affinity seems to cause an oxygen transfer from the base powder to the master alloy through the atmosphere. Such interaction is affected by the chemical composition of the base powder. Depending on the amount and type of oxides present in the base powder, their reduction will take place in a different temperature range, and so will do the internal-getter effect. If the internal-getter effect takes place at higher temperatures—as in the case of using Cr prealloyed as base powder—oxides with very high stability (Mn-Si or Si oxides) will be formed predominantly.

3. Lower oxygen contents are obtained in steels sintered in H_2 since the less stable iron oxides are reduced by H_2 at low temperatures—~673 K (400 °C)—at which the reactivity of the oxidation-sensitive elements is still scarce. However, formation of CH_4 is observed in the intermediate temperature range between 973 K and 1173 K (700 °C and 900 °C) and could be related with the oxidation of oxide-sensitive metals by reaction with CO and H_2. Thermodynamic calculations suggest that the use of diluted H_2 atmospheres should be the most effective way to avoid decarburization due to methane formation.

REFERENCES

1. L. Albano-Müller, F. Thümmler, and G. Zapf: *Powder Metall.*, 1973, vol. 16, pp. 236–56.
2. G. Zapf and K. Dalal: *Mod. Dev. Powder Metall.*, 1977, vol. 10, pp. 129–152.
3. H. Danninger and C. Gierl: *Sci. Sinter.*, 2008, vol. 40, pp. 33–46.
4. M. Jaliliziyaean, C. Gierl, and H. Danninger: *Adv. Powder. Metall. Part. Mater.*, 2008, vol. 5, pp. 72–78.
5. H. Danninger, M. Jaliliziyaeian, C. Gierl, and S. Bengtsson: *Mater. Sci. Forum*, 2011, vol. 672, p. 4.
6. E. Hryha, C. Gierl, L. Nyborg, H. Danninger, and E. Dudrova: *Appl. Surf. Sci.*, 2010, vol. 256, pp. 3946–61.
7. S. Banerjee, G. Schlieper, F. Thümmler, and G. Zapf: *Prog. Powder Metall.*, 1980, vol. 13, pp. 143–57.
8. G. Schlieper and F. Thummler: *Powder Metall. Int.* 1979, pp. 172, 174–76.
9. P. Jones and R. Lawcock: Stackpole Limited, US, 1997.
10. P. Jones and R. Lawcock: Stackpole Limited, US, 1999.
11. F. Castro, M. Sarasola, F. Baumgaertner, M. Dougan, S. Mitchell, K. Lipp, H.J. Bender, C. Coffin, and J. Dunkley: *EuroPM2005*, EPMA, ed. EPMA, Pragha, 2005.
12. P. Beiss: *Adv. Powder Metall. Part. Mater.*, 2006, vol. 1, pp. 12–20.
13. S. Sainz, V. Martinez, M. Dougan, F. Baumgaertner, and F. Castro: *Adv. Powder Metall. Part. Mater.*, 2006, vol. 7, pp. 95–108.
14. A. Šalak and M. Selecká: *Manganese in Powder Metallurgy Steels*, Cambridge International Science, Cambridge, 2012.
15. A.N. Klein, R. Oberacker, and F. Thummler: *Powder Metall. Int.*, 1985, vol. 17, pp. 13–16.
16. A.N. Klein, R. Oberacker, and F. Thummler: *Powder Metall. Int.*, 1985, vol. 17, pp. 71–74.
17. A.N. Klein, R. Oberacker, and F. Thummler: *Mod. Dev. Powder Metall.*, 1985, vol. 16, pp. 141–52.
18. F. Thummler, A. Klein, and R. Oberacker: Kernforschungszent Karlsruhe, 1983.
19. F. Thummler, A. Klein, and R. Oberacker: Kernforschungszent Karlsruhe, 1990.
20. R. Oro, M. Campos, J.M. Torralba, and C. Capdevila: *Powder Metall.*, 2012, vol. 55, pp. 294–301.
21. M.C. Abraham and A. Ghosh: *Symposium on Science and Technology of Sponge Iron and Its Conversion to Steel*, CSIR—National Metallurgical Laboratory, Jamshedpur, 1973, pp 106–16.
22. D.M. dos Santos and M.B. Mourao: *Scand. J. Metall.*, 2004, vol. 33, pp. 229–35.
23. H. Danninger, G. Frauendienst, K.D. Streb, and R. Ratzi: *Mater. Chem. Phys.*, 2001, vol. 67, pp. 72–77.
24. H. Danninger and C. Gierl: *Mater. Chem. Phys.*, 2001, vol. 67, pp. 49–55.
25. M. Momeni, C. Gierl, and H. Danninger: *Mater. Chem. Phys.*, 2011, vol. 129, pp. 209–16.
26. H. Danninger, C. Gierl, S. Kremel, G. Leitner, K. Jaenicke-Roessler, and Y. Yu: *Powder Metall. Prog.*, 2002, vol. 2, pp. 125–40.
27. H. Danninger, C. Gierl, G. Leitner, and K. Jaenicke-Roessler: *P/M Sci. Technol. Briefs*, 2004, vol. 6, pp. 10–14.
28. C. Gierl, M. Jaliliziyaean, H. Danninger, and S. Berngtsson: *Euro PM2009*, EPMA, ed., EPMA: Copenhague, 2009, pp 305–10.
29. A.P. Long, S.L. Li, H. Wang, and H.Z. Chen: *Appl. Surf. Sci.*, 2014, vol. 295, pp. 180–88.
30. R. Oro, M. Campos, E. Hryha, J.M. Torralba, and L. Nyborg: *Mater. Charact.*, 2013, vol. 86, pp. 80–91.
31. D. Chasoglou, E. Hryha, and L. Nyborg: *Mater. Chem. Phys.*, 2013, vol. 138, pp. 405–15.
32. E. Hryha, E. Dudrova, and L. Nyborg: *J. Mater. Process. Technol.*, 2012, vol. 212, pp. 977–87.
33. H. Danninger, M Jaliliziyaean, C. Gierl, E. Hryha, and S. Bengtsson: *World PM2010*, EPMA, ed., EPMA, Florence, Italy, 2010, pp. 3–10.
34. J.E. Japka: *J. Met.*, 1988, vol. 40, pp. 18–21.
35. E. Hryha and E. Dudrova: *Prog. Powder Metall.*, 2007, vols. 534–536 (1–2), pp. 761–64.
36. E. Hryha, E. Dudrova, and L. Nyborg: *Metall. Mater. Trans. A*, 2010, vol. 41A, pp. 2880–97.
37. B. Lindsley and W.B. James: *Adv. Powder Metall. Part. Mater.*, 2010, vol. 10, pp. 36–49.
38. K. Stölzel: *Technik-Wörterbuch Metallurgie und Gießereitechnik: russ., dt.*, Verlag Technik, 1986.
39. G. Jangg, R. Kieffer, and P. Ettmayer: *Sondermetalle*, Wien-New York, 1971.